International Journal of Scientific Engineering and Research (IJSER)
www.ijser.in
ISSN (Online): 2347-3878, Impact Factor (2015): 3.791

Latice Dynamical Study of Indium Arsenide (InAs)

Suresh Chandra Pandey[1], Kripa Shankar Upadhyaya[2]

[1]Department of Physics, Mahatma Gandhi Gramodaya Vishwavidyalaya, Chitrakoot, Satna M.P., India
[2]Department of Physics, Nehru Gram Bharti University, Allahabad, U.P., India

Abstract: ***The compound semiconductors of zinc-blende structures (ZBS) are the promising materials for numerous experimental and theoretical investigations. These investigations are the consequences of efforts devoted to understand the interesting crystal properties and interaction mechanism exhibited by these compounds. The complete lattice dynamics (phonon dispersion curves, Debye temperatures variation, combined density of states (CDS) curves, two-phonon Raman and anharmonic elastic properties) of InAs with zinc-blende structure has been investigated including van der Waal's interactions and three-body interactions into the rigid shell model of zinc blende structure, where the short range interactions are operative up to the second neighbours. Our results are in good agreement with the available measured data. It is concluded that this model VTSM will be equally applicable to study above properties of other zinc-blende structure solids as compared to the models of earlier workers.***

Keywords: Phonons, van der Waal's interactions, Debye temperatures variation, combined density of states curve, Raman spectra, Phonon dispersion curves, Lattice dynamics, InAs.

1. Introduction

In Recent past, considerable effort has been made to study the lattice dynamics of III-V compounds semi conductors having zinc blend structure, Such effort is possible due to availability of phonon frequencies by neutron scattering experiments [1], thermal diffuse scattering [2] and Raman spectra of InAs [3]. This particular attention is due to their high symmetry and simplicity of their ionic bonding. The semiconductor crystal InAs has remarkable property of transverse acoustic (TA) vibrations. The theoretical models used so far are rigid ion model and shell model.

The detailed collection of such models is given by Kunk etal (1975) [4] theoretical study of lattice dynamics of InAs has been made by Talwar and Agrawal (1974) [5] and Banarjee and Varshmi (1969) [6]. Using rigid ion model. Shell model has been used to study of lattice dynamics of number of f.c.c and b.c.c solids by Thakur and Singh (1986, 1987) [7,8] and Mishra and Singh (1988) [9]. Borcherds and Kunc (1978) [1] used an overlap-valance-shell model (OVSM).

In this paper phenomenological model called VTSM, we are mainly cancered with the lattice dynamical study of indium arsenide (InAs) the experimental data of InAs for phonon dispersion curve [11], harmonic and anharmonic elastic constants [12], Debye temperature variation [13-15] and Raman Spectra [3] are available. These workers have tried to interpret the phonon dispersion curves (PDCs) but none has succeeded in describing the PDC and other results of InAs very well. They have compared their theoretical results with their measured data but with only partial success.

Furthermore, effect of long range (LR) three body interactions (TBI), short range interaction Vander Waal's (VDW) attractions are significant in partially ionic and covalent crystal [16] though vander Waal's interaction, have much effective force, but Singh and Singh [17] have used only three body force shell model (TSM) formulation for InAs, InSb, InP without inclusion of vander Waal's interaction (VDWI). So far the calculation of third order elastic constant (TOEC) and pressure derivatives of second order elastic constant (SOEC) are concerned, Sharma and Verma [18] have reformulated the expression derived by Garg et. al. [19]. They have derived the correct expression for TOEC and pressure derivatives of SOEC for ZBS crystals. The various co-researchers (Upadhyaya et. al. [20, 21] Tiwari et. al. [22], Srivastava and Upadhyaya [23], Mishra and Upadhyaya [24], Dubey et. al. [25, 26]) used their correct expressions for calculating the anharmonic elastic properties for NaCl, CsCl and ZBS structure of solids, Therefore we have used expressions of Sharma and Verma [18] as such for our computations.

The above information have encouraged us to include (i) the effect of VDWI and (ii) TBI in the frame work of RSM where short range interactions are effective up to the second neighbours, Our model, thus developed is known as vander Waal's three body force shell model (VTSM). If has 14-parameters; four TBI parameters $b, \rho, f(r_0), r_0 f'(r_0)$; six nearest and next nearest neighbour short range repulsive interaction parameters $(A_{12}, B_{12}, A_{11}, B_{11}, A_{22}, B_{22})$, two distortion polarizabilities of negative and positive ions (d_1, d_2) and two shell charges of the negative and positive ions (Y_1, Y_2) respectively. They can be deduced with the help of measured values of elastic constants, dielectric constants, electronic polarizabilities and van der Waal's coupling coefficients. This model has been applied to study the lattice dynamics of indium pnictides (InP, InAs, InSb). In this paper, we are reporting the study of phonon dispersion curves, Debye temperatures variation, combined density of states (CDS), third order elastic constants and pressure derivatives of SOEC of InAs only. The formalism of our model has been presented in the next section in detail.

2. Theoretical Framework of the Present Model

We have developed a model for ZBS structure, which includes the effect of van der Waal's interactions (VDWI) and three body interactions (TBI) in the frame work of rigid shell model (RSM) where short range interactions are

effective upto the second neighbours and known as van der Waal's three body force shell model (VTSM).

2.1. Secular equations:

For ZBS crystals, the cohesive energy for a particular lattice separation (r) has been expressed as

$$\Phi(r) = \Phi_{LR}(r) + \Phi_{SR}(r) \quad (1)$$

where the first term $\Phi_{LR}(r)$ represent the long-range Coulomb and three body interaction (TBI) energies expressed by

$$\Phi_{LR}(r) = -\sum_{\substack{ij \\ i\neq j\neq k}} \frac{Z_i Z_j e^2}{r_{ij}}\left\{1+\sum_k f(r_{ik})\right\} = -\frac{\alpha_M Z^2 e^2}{r}\left\{1+\frac{4}{Z}f(r)\right\} \quad (2)$$

where Z_i is the ionic charge parameter of i^{th} ion, r_{ij} separation between i^{th} and j^{th} ion, $f(r_{ik})$ is the three-body force parameter dependent on nearest-neighbour separation r_{ik} and is a measure of ion size difference Singh [16], α_M is Madelung constant (=1.63805 for ZBS). The second term in equation (1) is short-range energy contributions from overlap repulsion and van der Waals interactions (VDMI) expressed as [27].

$$\Phi_{SR}(r) = Nb\sum_{i,j=1}^{2}\exp\left[\frac{r_i + r_j - r_{ij}}{\rho}\right] - \sum_{ij}\frac{c_{ij}}{r_{ij}^6} - \sum_{ij}\frac{d_{ij}}{r_{ij}^8} \quad (3)$$

where N is the Avogadro's a number, b is the hardness parameter and the first term is the Hafemeister and Flygare (HF) potential [31] and used by Singh and coworkers. The second term and third term represent the energy due to VDW for c_{ij} dipole-dipole (d - d) and d_{ij} dipole - quadrupole (d - q) interactions, respectively.

Using the crystal energy expression (1), the equations of motion of two cores and two shells can be written as;

$$\omega^2 \underline{M}\underline{U} = (\underline{R} + \underline{Z_m}\underline{C'}\underline{Z_m})\underline{U} + (\underline{T} + \underline{Z_m}\underline{C'}\underline{Y_m})\underline{W} \quad (4)$$

$$0 = (\underline{T}^T + \underline{Y_m}\underline{C'}\underline{Z_m})\underline{U} + (\underline{S} + \underline{K} + \underline{Z_m}\underline{C'}\underline{Y_m})\underline{W} \quad (5)$$

Here $\underline{U}$ and $\underline{W}$ are vectors describing the ionic displacements and deformations, respectively. $\underline{Z_m}$ and $\underline{Y_m}$ are diagonal matrices of modified ionic charges and shell charges, respectively; $\underline{M}$ is the mass of the core; $\underline{T}$ and $\underline{R}$ are repulsive Coulombian matrices respectively; $\underline{C'}$ are long-range interaction matrices that include Coulombian and TBI; $\underline{S}$ and $\underline{K}$ are core-shell and shell-shell repulsive interaction matrices, respectively and $\underline{T}^T$ is the transpose of matrix $\underline{T}$. The elements of matrix $\underline{Z_m}$ consist of the parameter Z_m giving the modified ionic charge.

$$Z_m = \pm Z\sqrt{1+\left(\frac{8}{z}\right)f(r_0)} \quad (6)$$

The elimination of $\underline{W}$ from eqns. (4) and (5) leads to the secular determinant;

$$\left|\underline{D}(\vec{q}) - \omega^2 \underline{M}\underline{I}\right| = 0 \quad (7)$$

for the frequency determination. Here $\underline{D}$ (q) is the (6 × 6) dynamical matrix given by

$$\underline{D}(\vec{q}) = (\underline{R} + \underline{Z_m}\underline{C'}\underline{Z_m}) - (\underline{T} + \underline{Z_m}\underline{C'}\underline{Y_m}) \times (\underline{S} + \underline{K} + \underline{Y_m}\underline{C'}\underline{Y_m})^{-1}(\underline{T}^T + \underline{Y_m}\underline{C'}\underline{Z_m}) \quad (8)$$

The numbers of adjustable parameters have been largely reduced by considering all the short-range interactions to act only through the shells.

2.2. Vibrational Properties of Zinc-Blende Structure:

By solving the secular equation (4) along [q 0 0] direction and subjecting the short and long-range coupling coefficients to the long-wavelength limit $\vec{q} \to 0$, two distinct optical vibration frequencies are obtained as

$$(\mu\omega_L^2)_{q=0} = R_0' + \frac{(z'e)^2}{vfL}.\frac{8\pi}{3}\left(Z_m^2 + 4Zr_0 f'(r_0)\right) \quad (9)$$

$$(\mu\omega_T^2)_{q=0} = R_0' - \frac{(z'e)^2}{vfT}.\frac{4\pi}{3}Z_m^2 \quad (10)$$

where the abbreviations stand for

$$R_0' = R_0 - e^2\left(\frac{d_1^2}{\alpha_1} + \frac{d_2^2}{\alpha_2}\right); R_0 = \frac{e^2}{v}\left[4\frac{A_{12}+2B_{12}}{3}\right]; Z' = Z_m + d_1 - d_2 \quad (11)$$

$$f_L = 1 + \left(\frac{\alpha_1+\alpha_2}{v}\right).\frac{8\pi}{3}\left(Z_m^2 + 4Zr_0 f'(r_0)\right) \quad (12)$$

$$f_T = 1 - \left(\frac{\alpha_1+\alpha_2}{v}\right).\frac{4\pi}{3} \quad (13)$$

and

$$\alpha = \alpha_1 + \alpha_2 \quad (14)$$

and $v = 3.08r_0^3$ for ZBS (volume of unit cell).

2.3. Debye Temperatures Variation:

The specific heat at constant volume C_v at temperature T is expressed as

$$C_v = 3NK_B \frac{\int_0^{v_m}\left\{\left(\frac{hv}{K_BT}\right)^2 e^{hv/K_BT}\right\}G(v)dv \Big/ (e^{hv/K_BT}-1)^2}{\int_0^{v_m} G(v)dv} \quad (15)$$

where, v_m is the maximum frequency, h is the Planck's constant and K_B is the Boltzmann's constant. The equation (15) can be written as a suitable form for a computational purpose as

$$C_v = 3NK_B \frac{\sum_v \{E(x)\}G(v)dv}{\sum_v G(v)dv} \quad (16)$$

where E(x) is the Einstein function, defined by

$$E(x) = x^2 \frac{\exp(x)}{\{\exp(x)-1\}^2} \quad (17)$$

where $x = \left\{ \left(\frac{h\nu}{K_B T} \right)^2 e^{\frac{h\nu}{K_B T}} \right\}$

Also, $\sum_\nu G(\nu)d\nu =$ Total number of frequencies considered.
= 6000 for zinc-blende structure.

Hence, equation (16) can be written for zinc-blende structure type crystals, as

$$C_v = \frac{3NK_B}{6000} \sum_\nu E(x)G(\nu)d\nu \quad (18)$$

The contribution of each interval to the specific heat is obtained by multiplying an Einstein function corresponding to mid-point of each interval (say 0.1 THz) by its statistical weight. The statistical weight of the interval is obtained from the number of frequencies lying in that interval. The contributions of all such intervals, when summed up give, $\sum_\nu E(x)G(\nu)d\nu$. The Specific heat C_v is then calculated by expression (18).

2.4. Second and third order elastic constant:

Proceeding with the use of three body crystal potential given by equation (1), (Sharma and Verma [18]) have derived the expressions for the second order elastic constants and used by (Singh and Singh [17]) for zinc-blende structure crystals. We are reporting them here as their corrected expressions.

The expressions for second order elastic constants (SOEC) are;

$$C_{11} = L\left[0.2477Z_m^2 + \frac{1}{3}(A_1 + 2B_1) + \frac{1}{2}(A_2 + B_2) + 5.8243Zaf'(r_0) \right] \quad (19)$$

$$C_{12} = L\left[-2.6458Z_m^2 + \frac{1}{3}(A_1 - 4B_1) + \frac{1}{4}(A_2 - 5B_2) + 5.8243Zaf'(r_0) \right] \quad (20)$$

$$C_{44} = L\left[-0.123Z_m^2 + \frac{1}{3}(A_1 + 2B_1) + \frac{1}{4}(A_2 + 3B_2) - \frac{1}{3}\nabla(-7.539122Z_m^2) + A_1 - B_1 \right] \quad (21)$$

where $A_1 = A_{12}, B_1 = B_{12}, A_2 = A_{11} + A_{22}, B_2 = B_{11} + B_{22}, \mathrm{C}_1 = \frac{A_{12}^2}{B_{12}}$ and $\mathrm{C}_2 = \frac{A_2^2}{B_2}$

and the expressions for third order elastic constants (TOEC) are-

$$C_{111} = L\left[\begin{array}{l} 0.5184Z_m^2 + \frac{1}{9}(C_1 - 6B_1 - 3A_1) + \frac{1}{4}(C_2 - B_2 - 3A_2) - 2(B_1 + B_2) - \\ 9.9326Zaf'(r_0) + 2.5220Za^2 f''(r_0) \end{array} \right] \quad (22)$$

$$C_{112} = L\left[\begin{array}{l} 0.3828Z_m^2 + \frac{1}{9}(C_1 + 3B_1 - 3A_1) + \frac{1}{8}(C_2 + 3B_2 - 3A_2) - 11.642Zaf'(r_0) + \\ 2.5220Za^2 f''(r_0) \end{array} \right] \quad (23)$$

$$C_{113} = L\left[6.1585Z_m^2 + \frac{1}{9}(C_1 + 3B_1 - 3A_1) - 12.5060Zaf'(r_0) + 2.5220Za^2 f''(r_0) \right] \quad (24)$$

$$C_{144} = L\left[\begin{array}{l} 6.1585Z_m^2 + \frac{1}{9}(C_1 + 3B_1 - 3A_1) - 4.1681Zaf'(r_0) + 0.8407Za^2 f''(r_0) + \\ \nabla\left\{ -3.3507Z_m^2 - \frac{2}{9}C_1 + 13.5486af'(r_0) - 1.681a^2 f''(r_0) \right\} + \\ \nabla^2\left\{ -1.5637Z_m^2 + \frac{2}{3}(A_1 - B_1) + \frac{C_1}{9} - 5.3138Zaf'(r_0) + 2.9350Za^2 f''(r_0) \right\} \end{array} \right] \quad (25)$$

$$C_{166} = L\left[\begin{array}{l} -2.1392Z_m^2 + \frac{1}{9}(C_1 - 6B_1 - 3A_1) + \frac{1}{8}(C_2 - 5B_2 - 3A_2) - (B_1 + B_2) - \\ 4.1681Zaf'(r_0) + 0.8407Za^2 f''(r_0) + \\ \nabla\left\{-8.3768Z_m^2 + \frac{2}{3}(A_1 - B_1) - \frac{2}{9}C_1 + 13.5486af'(r_0) - 1.681a^2 f''(r_0)\right\} + \\ \nabla^2\left\{2.3527Z_m^2 + \frac{1}{9}C_1 - 5.3138Zaf'(r_0) + 2.9350Za^2 f''(r_0)\right\} \end{array}\right] \quad (26)$$

$$C_{456} = L\left[\begin{array}{l} 4.897Z_m^2 + \frac{1}{9}(C_1 - 6B_1 - 3A_1) - B_2 + \\ \nabla\left\{-5.0261Z_m^2 - \frac{1}{9}C_1\right\} + \nabla^2\left\{7.0580Z_m^2 + \frac{1}{3}C_1\right\} + \\ \nabla^3\left\{-4.8008Z_m^2 + \frac{1}{3}(A_1 - B_1) - \frac{1}{9}C_1\right\} \end{array}\right] \quad (27)$$

where Z_m is the modified ionic charge defined earlier with $L = \frac{e^2}{4a^4}$ and

$$\nabla = \left[\frac{-7.53912Z(Z + 8f(r_0)) + (A_1 - B_1)}{-3.141Z(Z + 8f(r_0)) + (A_1 + 2B_1) + 21.765Zaf'(r_0)}\right] \quad (28)$$

and Pressure derivatives of SOEC

$$\frac{dK'}{dP} = -(3\Omega)^{-1}\left[\begin{array}{l} 20.1788Z_m^2 + 3(A_1 + A_2) + 4(B_1 + B_2) + (C_1 + C_2) - 104.8433Zaf'(r_0) \\ +22.7008Za^2 f''(r_0) \end{array}\right] \quad (29)$$

$$\frac{dS'}{dP} = -(2\Omega)^{-1}\left[\begin{array}{l} -11.5756Z_m^2 + 2(A_1 - 2B_1 + \frac{3A_2}{2} - \frac{7B_2}{2} + \frac{1}{4}\cdot C_2 + \\ 37.5220Zaf'(r_0) \end{array}\right] \quad (30)$$

$$\begin{aligned} \frac{dC'_{44}}{dP} = -(\Omega)^{-1}\Bigg[& \left\{0.4952Z_m^2 + \frac{1}{3}(A_1 - 4B_1 + C_1) + \frac{1}{2}\cdot A_2 - \frac{3}{2}\cdot B_2 + \frac{1}{4}\cdot C_2 + 4.9667Zaf'(r_0)\right. \\ & \left. +2.522Za^2 f''(r_0)\right\} \\ & +\nabla\left\{-17.5913Z_m^2 + A_1 - B_1 - \frac{2}{3}\cdot C_1 + 40.6461Zaf'(r_0) + 5.044Za^2 f''(r_0)\right\} \\ & +\nabla^2\left\{3.1416Z_m^2 + \frac{2}{3}(A_1 - B_1) + \frac{1}{3}\cdot C_1 - 15.9412Zaf'(r_0)\right. \\ & \left. +8.8052Za^2 f''(r_0)\right\}\Bigg] \end{aligned} \quad (31)$$

where $K = \frac{C_{11} + 2C_{12}}{3}, S = \frac{C_{11} - C_{22}}{2}$

and $\Omega = -5.0440Z_m^2 + (A_1 + A_2) - 2(B_1 + B_2) + 17.4730Zaf'(r_0)$

The values of *Ai*, *Bi* and *Ci* as defined by Sharma and Verma [18].

3. Computations

The model parameters (b, ρ and $f(r_0)$), have been determined by using the expressions (19-21) and the equilibrium condition

$$\left(\frac{d\Phi(r)}{dr}\right)_{r_0 = a\frac{\sqrt{3}}{2}} = 0,$$

with the inclusion of the van der Waal's interactions (VDWI) [equation (3)]. The value of the input data [11, 12, 29-31, 32] and model parameters have been shown in Table 1. The value of A_i, B_i, C_i have been calculated from knowledge of b, ρ; the value of various order of derivatives

of $f(r_0)$ and van der Waal's coupling coefficient [18]. The values of VDW coefficients used by us in present study have been determined using the Slatre-Kirkwood variation (SKV) methods [33], Lee [34] approach as suggested by Singh and Singh [17] and reported by Sharma and Verma [18]. Thus our model parameters are [b, ρ, $f(r_0)$, $r_0f'(r_0)$, A_{12}, A_{11}, A_{22}, B_{12}, B_{11}, B_{22}, d_1, d_2, y_1 and y_2]. The values of the van der Waal's coefficient (VDW) are shown in table 2. Our model parameters of VTSM have been used to compute the phonon spectra of InAs for the allowed 48 non-equivalent wave vectors in the first Brillouin zone. The frequencies along the symmetry directions have been plotted against the wave vector to obtain the phonon dispersion curves (PDC). These curves have been compared with those measured by means of the coherent in elastic neutron scattering technique, thermal diffuse X-ray data [2] in figure1 along with OVSM calculation of Borcherds and K.Kunc [1]. Since the neutron scattering experiments provide us only very little data for symmetry directions, we have also computed combined density of states (CDS) and Debye temperature variation for the complete description of the frequencies for the Brillouin zone.

The complete phonon spectra have been used to compute the combined density of state (CDS), [35] $N(\nu_j + \nu_j')$ and $(\nu_j + \nu_j')$ has been plotted and smoothed out as shown in figure2. These curve shown will define peaks which correspond to two phonon Raman scattering. These CDS peaks have been compared with assignments calculated and shown in table-3. The Debye temperature variation for InAs measured from [13-15] and those calculated by using VTSM has been compared in figure3. The calculated value of TOEC using equation (22-27) have been compared with calculated value of Sadao Adachi [36] and shown in table 4. The pressure derivatives of SOEC also have been calculated and compared with those measured by [38-39]

4. Results and Discussion

4.1. Phonon Dispersion Curves:

From figure 1. our phonon dispersion curve for InAs agree with measured Raman data reported by carles et. al. [11]. It is evident from PDC that our predictions using present model (VTSM) are better than those by using OVSM [1]. Our model has successfully explained the dispersion of phonons along the three symmetry direction from figure 1 and table 6. It is clear that : there are deviations of 3.40% along TO(X), 18.7% along TA(X), 4.92% along LO(L), 2.94% along TO(L), 3.41% along LA(L) and 15.75% along TA(L) while from VTSM 0.46% along TO(X), 0.0% along LA(X), 0.98% along TA(X), 0.16% along LO(L), 0.46% along TO(L), 0.21% along LA(L) and 2.36% along TA(L) From table 6. it is clear that VTSM has very small deviation from experimental data. Our model has 17.72% improvement over OVSM due to inclusion of three body interactions (TBI) and VDWI coefficient, Therefore, our VTSM model has better agreement with experimental data over OVSM [1].

4.2. Combined density of States:

The present model is capable to predict the two phonon Raman spectra [3], the results of these investigations for combined density state (CDS) peaks have been presented in figure 2. The theoretical peaks are in good agreement with observed Raman peaks for InAs, the assignments made by the critical point analysis have been shown in table 3. The interpretations of Raman spectra achieved from both CDS approach and critical point analysis is quite satisfactory. This explains that there is an excellent agreement between experimental data and our theoretical results.

4.3. Third order elastic constants (TOEC) and pressure derivatives of second order elastic constants (SOEC):

It is interesting to note that our results on TOEC and pressure derivatives of SOEC for indium arsenide (InAs) as comparable to others are closer to their experimental values. The present models computation of third order elastic constants (TOEC) have been reported in table 4 and compared with available experimental data and theoretical results of Sadao Adachi [36]. Further, pressure derivatives of SOEC for InAs are compared with available experimental data [38, 39] in table 5. The results are in good agreement.

4.4. Debye temperature variations:

From figure 3, Our study shows a better agreement with the measured data [13-15] and theoretical results of valence force field model VFFM [40]. We can say that our present model gives a better interpretation of the Debye temperature variation for InAs.

5. Conclusion

The inclusion of van der waal's interaction (VDWI) with TBI have influenced both the optical branches and the acoustic branches. Another striking feature of present model is noteworthy from excellent reproduction of almost all branches of PDCs. Hence the prediction of phonon dispersion curves (PDC) for InAs using VTSM may be considered more satisfactory than from other model [17]. The basic aim of the study of two phonon Raman spectra are to correlate the neutron scattering and optical measured data of InAs. In this paper, we have systematically reported phonon dispersion curves, combined density of states, Debye temperature variation and a part of harmonic and anharmonic properties of InAs. On the basis of overall discussion, it is concluded that our van der Waal's three body force shell model (VTSM) is adequately capable of describing the crystal dynamics of indium arsenide. This model has been applied equally well to study the crystal dynamics of other compounds of this group (InP and InSb) and sent for publication elsewhere. Our work gets strong support from papers of Mishra and Upadhyaya [24] and Dubey et. al. [25, 26].

Acknowledgements

One of us Suresh Chandra Pandey is grateful to Dr. Bharat Mishra and Dr. Uma Shankar Mishra Mahatma Gandhi Gramodaya Vishwavidyalaya, Chitrakoot, Satna M.P., India for encouragement. Authors are also thankful to computer centre B.H.U. Varansi, India for providing computational assistance.

References

[1] P.H. Borcherds and K. Kunc, (1978) J. Phys. C11, 4145.
[2] Orlova, N.S. : (1983) Phys. Status Solidi (b) 119, 541.
[3] M. Cardona, in light scattering in solids, topics in applied physics, edited by M.Cardona (Springer, Berlin 1976) vol 8, P.I.
[4] Kunk K., Balkanskim, and Nusimonvici M.A., (1975) Phys. Status Solidi (b) 72, 229
[5] Talwar, D.N. and B.K. Agrawal (1974), Solid State Commun. 11 : 1691.
[6] Banarjee, R and Y.P. Varshni (1969), Cand J.Phys. 47, 451
[7] Thakur, V.K. and T.N. Singh (1986), Phys. Stat, Sol. (b) 135 : 67.
[8] Thakur, V.K. and T.N. Singh (1987), Phys. Stat, Sol (b) 142; 401
[9] Mishra, S.K. and T.N. Singh (1988), Phys. Stat. Sol (b) 149; 503
[10] Kaplan, H., Sullivan, J.J. (1969). Lattice vibrations of zinc-blende structure crystals. Phys. Rev., 130, 120.
[11] Carles, R., Saint-Cricq, N., Renucci, J.B., Renucci, M.A. Zwik, A. : (1980) Phys. Rev. B22, 4804
[12] Gray, D.W. (1972), American Institute of Physics hand book. 3rd ed.
[13] U. Piesbergen, (1966) Semiconductors and Semimetals 2, 49.
[14] N. N. Sirota, A.M. Antyukhov, V.V. Novikov, V.A. Fyodorov, (1982) Cryst. Res. Technol. **17**, 279.
[15] T.C. Cetas, C.R. Tilford, and C.A. Swenson, (1968) Phys. Rev. **174,** 835.
[16] Singh, R.K. (1982), Physics Reports (Netherlands), 85, 259.
[17] Singh, R.K. and Singh, S. (1987), Phys. Status Solidi (b) 140, 407
[18] Sharma, U. C. and Verma, M.P. (1980) Phys. Status Solidi (b) 102, 487
[19] Garg V.K., Puri D.S., Verma M.P. (1978) Phys. Status Solidi (b) 87, 401
[20] Upadhyaya K.S., Pandey A, Srivastava D. M. (2006) Chinese J. Phys. 44, 127
[21] Upadhyaya, K.S., Upadhyay, G.K., Yadav, M., Singh, A.K., (2001) J. Phys. Soc. Japan, 70, 723
[22] Tiwari, S.K., Pandey, L.K., Shukla, L.J., Upadhyaya, K.S., (2009) Phyica Scr., 80, 065603
[23] Srivastava, U.C., Upadhyaya, K.S., (2011) Physcial Rev. and Res. Int., 1, 16
[24] Mishra, K.K., Upadhyaya, K.S., (2012) Int., Jour. Sci. Engg. Res, 3, 1388
[25] Dubey J.P., Tiwari R.K., Upadhyaya K. S. and Pandey P.K., (2015) Turk. J. Phys. 39, 242
[26] Dubey J.P., Tiwari R.K., Upadhyaya K.S. and Pandey P.K., (2015) Jour. of Appl. Phys. (IOSR-JAP) 7, 67
[27] Singh R. K. and Khare P., (1982) J. Phys. Soc. Japan 51, 141
[28] Hafemeister D. W. and Flygare W. H.J., (1965) Chem. Phys. 43, 795
[29] Levinstein M, Rumyantsev S and Shur M 1990 hand book series on semiconductor parameters vol 1, 2 (London : world scientific)
[30] Kushwaha M.S. and Kushwaha S.S., (1980) cand J. Phys. 58, 351
[31] Price D.L., Row J.M. and nicklow R.M., (1971) Phys. Rev B3, 1268
[32] Shankar, J., Sharma, J.C., Sharma, D.P., (1977) Ind. Jour. Pure Appl. Phys., 15, 811.
[33] Slater J. C. and Kirkwood J.G., (1931) Phys. Rev. 37, 682
[34] Lee B.H.J., (1970) Appl. Phys. 41, 2988
[35] Smart C., Wilkinson G.R. and Karo A.M., Lattice Dynamics, edited by Wallis R.F. (1965)
[36] Sadao Adachi; Semiconductor Wiley series in materials for Electronic and opto electronic Application. Department of Electric Engineering Gunma University. Japan (1956)
[37] Land lots - born stein - group III. Condensed matter volume 44D2011.
[38] Yogurteu YK, mitter AJ, Saunders GA, (1981) J Phys. Chem solids, 42, 49.
[39] Soma, T., Kagaya, H. M.: (1983) Phys. Status Solidi (b) 118, 245.
[40] S.R.B thapa, Indian Journal of research (2011) 5, 47-54
[41] Yip, S., Chang, Y.: (1984) Phys. Rev. B 30, 7037

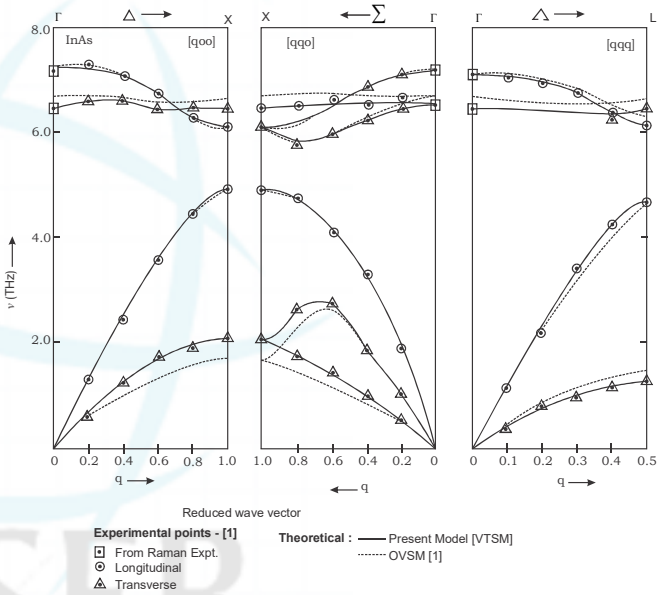

Fig.1 Phonon dispersion curves for InAs.

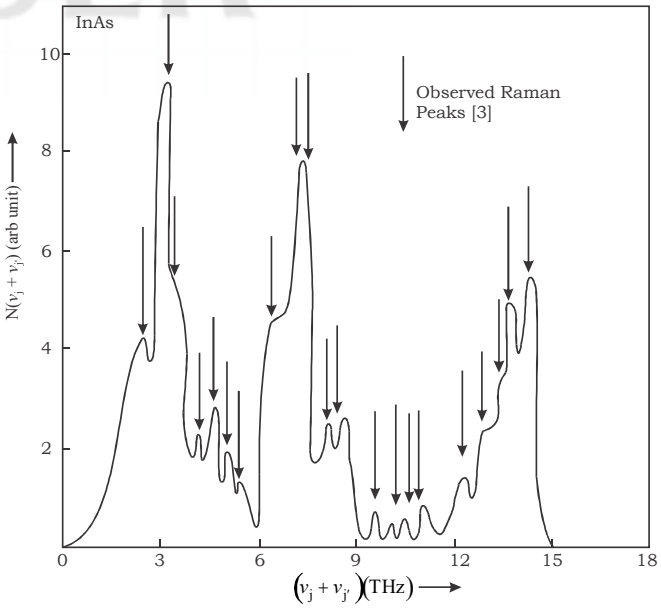

Fig.2 : Combined density of states curve for InAs

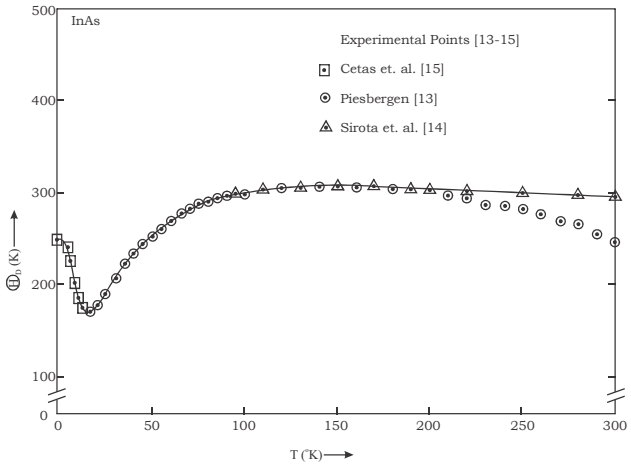

Fig.3 : Debye characteristic temperature Θ_D (°K) as a function of temperature T for InAs

Table 1: Input data and model parameters for InAs [C_{ij} and B (in 10^{11} dyne/cm^2), v in (THz), r_0 (in 10^{-8} cm), α_i (in 10^{-24} cm^3), b (in 10^{-12} erg), ρ (in 10^{-8} cm)]

Input Data		Model Parameter	
Properties	Values	Parameters	Values
C_{11}	8.329[a]	B	1.47
C_{12}	4.526[a]	ρ	0.56
C_{44}	3.959[a]	f (r_0)	–0.26
B	–5.79[b]	$r_0 f'(r)$	1.2117
r_0	2.61[a]	A_{12}	12.71
v LO (Γ)	7.38[f]	B_{12}	–6.78
v TO (Γ)	6.63[f]	A_{11}	58.51
v LO (L)	6.89[f]	B_{11}	–26.18
v TO (L)	6.47[f]	A_{22}	20.52
v LA (L)	4.69[f]	B_{22}	–14.27
v TA (L)	1.27[f]	d_1	0.1369
α_1	0.221[d]	d_2	2.8569
α_2	7.50[e]	Y_1	–0. 7152
ϵ_0	12.3[c]	Y_2	–2.1456
ϵ_∞	15.15[c]		

Ref.:
(a) [12]
(b) [31]
(c) [29]
(d) [3]
(e) [32]
(f) [11]

Table 2: van der Waal's Interaction Coefficients for InAs
(C_{ij} and C in units of 10^{-60} erg cm^6 and d_{ij} and D in units of 10^{-76} erg cm^8)

Parameters	Numerical Values
C_{+-}	671
C_{++}	401
C_{--}	1208
d_{+-}	490
d_{++}	205
d_{--}	1077
C	3535
D	2160

Table 3: Assignments for the observed peak positions in Combined Density of States in terms of selected phonon frequencies at Γ, X and L critical point for InAs

CDS Peaks (cm^{-1})	Raman Active		
	Observed Raman Peaks (cm^{-1}) [1, 3]	Present Study	
		Values (cm^{-1})	Assignments
88	87.5	86	2TA (L)
108	106.5	107	LO-LA (Δ)
115	112	114	LA-TA (L)
142	143	136	2TA (X)
154	157	158	TO-TA (Δ)
167	165	168	LO-TA (Δ)
177	176	175	LA+TA (Δ)
220	217.3	200	LA + TA (L)
240	238.6	236	2LA (Δ)
.....	253	.....	.....
272	270	271	LO + TA (X)
279	279	282	LO + TA (Δ)
328	320	314	2LA (L)
338	343	343	LO + LA (Δ)
350	356	.....	.....
367	365	368	LO + LA (X)
410	409	406	2LO (X) 2LO (L)
434	432	433	2TO (X) 2TO (L)
443	445	444	2TO (Γ)
455	456.5	450	2 LO (Δ)
482	479	494	2LO (Γ)

Table 4: Third Order Elastic Constants (in the unit of 10^{11} dyne/cm^2) for InAs

Property	Present Study	Other Theoretical Results [36]
C_{111}	–5.373	–3.56
C_{112}	–2.272	–2.66
C_{123}	–1.790	–1.00
C_{144}	–1.706	+0.16
C_{166}	–0.940	–1.39
C_{456}	–0.190	–0.004

Table 5: Values of pressure derivatives of SOEC (in dimensionless) for InAs

Property	Present Study	Experimental [39]	**Other [38]**
$\frac{dK'}{dP}$	3.74	2.79	3.40
$\frac{dS'}{dP}$	0.80	0.78	0.67
$\frac{dC'_{44}}{dP}$	0.56	0.41	0.46

Table 6: Comparison of Frequencies from Various Sources (X and L points) for InAs

Point	**Branches**	**Expt. [1] (THz)**	**OVSM [17]**			**Present study**			**% Improvement over OVSM (a ~ b)**
			Value (THz)	**(±) Deviation**	**% (a)**	**Value**	**(±) Deviation**	**% (b)**	
X (100)	LO	6.09	6.09	0.00	0.0	6.10	.01	0.16	0.16
	TO	6.47	6.69	0.22	3.40	6.50	.03	0.46	2.94
	LA	4.95	4.95	0.00	00	4.95	0.00	00	00
	TA	2.03	1.65	0.38	18.7	2.05	.02	0.98	17.72
L (.5.5.5)	LO	6.09	6.39	0.30	4.92	6.10	.01	0.16	4.76
	TO	6.47	6.66	0.19	2.94	6.50	.03	0.46	2.48
	LA	4.69	4.53	0.16	3.41	4.7	.01	0.21	3.2
	TA	1.27	1.47	0.20	15.75	1.30	.03	2.36	13.39